



Isothermal and non-isothermal crystallization kinetics of PLA/PBS blends with talc as nucleating agent

Runglawan Somsunan^{1,2} · Narinya Mainoiy¹

Received: 3 October 2018 / Accepted: 24 July 2019 / Published online: 8 August 2019
© Akadémiai Kiadó, Budapest, Hungary 2019

Abstract

The isothermal and non-isothermal crystallization kinetics of PLA/PBS at the blend ratio of 90/10 by mass containing 0.1% of talc was studied by differential scanning calorimetry. In this study, Avrami and Tobin equations were used to explain isothermal crystallization kinetics. The results of both theoretical models offered the same trend results which were the different crystallization temperatures influenced crystallization rate and the amount of crystallinity. It was found that at 100 °C is the temperature for the fastest of the completion of the crystallization blending process. Both models were also used to calculate the overall kinetic rate constant, n value, half-time of crystallization and growth rate. They indicated that growth dimension was three-dimensional which is the spherulitic growth from instantaneous nuclei of heterogeneous nucleation and occurred from talc. For non-isothermal crystallization kinetics, Jeziorny and Ozawa equations were used to explain. The results from Jeziorny equation show that there are two stages of crystallization at high cooling rate, the straight line in the primary stage followed by the nonlinear line in the secondary stage. It was also found that Jeziorny crystallization rate increased when the cooling rate increased. However, the Ozawa model was inappropriate for describing the non-isothermal crystallization for these blends.

Keywords Isothermal crystallization · Non-isothermal crystallization · Poly(lactic acid) · Poly(butylene succinate) · Talc · Nucleating agent

Introduction

Currently, biodegradable polymer has an important role for better life. Many studies have been studied how to improve their applications by improving the properties of the polymer to achieve the specific property requirement. Poly(lactic acid), PLA, is a polymer which received much commercial attention because of its biodegradability, good biocompatibility, and high strength [1–3]. In particular, it produces from renewable raw materials. Nevertheless, with some disadvantages which are brittleness and low crystallization rate, so it cannot be used in some applications. To solve this problem, the blending PLA with other polymers

is one of the most used methods because it can control the properties of the blends by adjusting their compositions to get the desired properties. Examples of these polymers are polycaprolactone, PCL [4, 5], poly(butylene adipate-co-terephthalate), PBAT [6] and poly(butylene succinate-co-adipate), PBSA [7].

Among these, polymer that has been one of the most attention and interest to be studied in this research for improving the properties of PLA is poly(butylene succinate), PBS. PBS has high flexibility and a high crystallization rate which allows high-speed industrial process. Hassan et al. [8] studied the blends of PLA and PBS with various compositions. The result showed that thermal stability of the blends was higher than that of pure PLA. The tensile strength and modulus of the blends decreased with the increasing of PBS content. Addition of PBS in PLA decreased the brittleness and elongation properties of the blends. It is clear that the addition of PBS up to 20% by mass in the blend was appropriate to be used as fibers and the 60% by mass of PBS in the blends would be suitable for

✉ Runglawan Somsunan
runglawan.s@cmu.ac.th

¹ Department of Chemistry, Faculty of Science, Chiang Mai University, Chiang Mai 50200, Thailand

² Center of Excellence in Materials Science and Technology, Chiang Mai University, Chiang Mai 50200, Thailand

packaging applications. Bhatia et al. [9] studied the PLA/PBS blends, and it was a miscible blend at up to 80/20 by mass composition.

Generally, improving the crystallization rate and morphology of polymer can be achieved by adding nucleating agents. In this study, Talc has chosen for use as nucleating agent. There have been reported that it has ability to be an efficacious nucleating agent. Li and Huneault [10] studied the effect of heterogeneous nucleation on PLA by adding 1% by mass of talc, 1% by mass of calcium lactate and 0.5% by mass of sodium stearate as nucleating agents and 5 and 10% by mass of PEG as plasticizers. The isothermal data showed that talc is highly effective in nucleating the PLA in the temperature range of 80–120 °C. The non-isothermal data showed that the combination of nucleating agent and plasticizer is necessary to develop significant crystallinity at high cooling rate. Moreover, Battezzore et al. [11] studied thermal properties of PLA with talc and the result showed that PLA did not crystallize unless adding talc as nucleating agent. They were found that talc can decrease the crystallization temperature about 23 °C and the amount of crystallinity increased higher than that of pure PLA after cooling. The amount of crystalline phase increased from 2.7 to 9.1% as increasing of talc content from 1 to 15% by mass. Kinetics of crystallization process was described by using Avrami equation. The result showed that micro-composite of PLA/talc had two-dimensional of growth kinetics as epitaxial growth. Mechanical property results showed that addition 5% by mass of talc increased modulus which was a result of the reinforcement of talc. However, the amount of talc which less than 5% by mass did not affect the modulus.

Theoretical modeling of isothermal crystallization kinetics

Isothermal crystallization kinetics based on the Avrami model [12–15]

A theoretical model of Avrami was used to describe the kinetics of crystallization for the substance under the conditions of constant temperature from the assumption that the number of nucleation nuclei is formed randomly on the area and the expansion or the growth of the nucleus, with a radius equal nucleus. The Avrami equation that used to describe the isothermal crystallization process in polymers is shown as following Eq. (1):

$$\alpha(t) = [1 - \exp(-K_A t^{n_A})] \quad (1)$$

where $\alpha(t)$ is the fraction of the crystallized material at time t , K_A is the Avrami crystallization rate and n_A is the Avrami constant. In general, the Avrami equation is often

converted into the traditional linear form as following Eq. (2):

$$\ln[-\ln(1 - \alpha(t))] = \ln(K_A) + n_A \ln(t) \quad (2)$$

The higher value of K_A means faster crystallization and the lower one takes longer time to crystallize. The n_A value depends on the growth dimension and type of nucleation. The n_A and K_A values are obtained from the slope and interception on the y-axis of the graph from the relationship between $\ln[-\ln(1 - \alpha(t))]$ versus $\ln(t)$.

The half-time of crystallization, $t_{1/2}$, is obtained from following Eq. (3)

$$t_{1/2} = (\ln(2)/K_A)^{1/n_A} \quad (3)$$

Typically, $t_{1/2}$ is often used to characterize the rate of crystallization directly. Moreover, the growth rate of the crystal (G) can be explained by the inverse of $t_{1/2}$ as following Eq. (4):

$$G = 1/t_{1/2} \quad (4)$$

Isothermal crystallization kinetics based on the Tobin model [15, 16]

Tobin's theory is a model that shows the development model of the Avrami equation. Tobin's equation is shown as follows (5):

$$\alpha(t) = (K_T t)^{n_T} / [1 + (K_T t)^{n_T}] \quad (5)$$

where $\alpha(t)$ is the fraction of crystallized material at time t , K_T is Tobin crystallization rate which independent on size of crystalline and Tobin constant (n_T). In addition, n_T is controlled directly by the different types of nuclei and growth mechanisms. The Tobin equation is generally often converted into the traditional linear form as following Eq. (6):

$$\log(\alpha_t/(1 - \alpha_t)) = \log(K_T) + n_T \log(t) \quad (6)$$

The n_T and K_T values are obtained from the slope and interception on the y-axis of the graph from the relationship between $\log(\alpha_t/(1 - \alpha_t))$ versus $\log(t)$.

Theoretical modeling of non-isothermal crystallization kinetics

The Avrami equation is the most widely used to describe isothermal crystallization kinetics. However, it is not appropriate for non-isothermal crystallization in which the temperature constant changes and the complexity of non-isothermal crystallization such as nucleation and temperature-crystal growth dependent [12]. Then, the Avrami

equation is improved to be explaining with non-isothermal crystallization.

For non-isothermal crystallization, time of crystallization can be calculated as following Eq. (7):

$$t = (T_o - T)/\varphi \quad (7)$$

where t is time of crystallization, T_o is the initiate temperature of crystallization and T is the temperature at time t and φ is cooling rate ($^{\circ}\text{C min}^{-1}$).

Non-isothermal crystallization kinetics based on the Jeziorny model [12, 13, 17–19]

Jeziorny explains non-isothermal crystallization by modification the theoretical models of Avrami. Jeziorny suggested that the Jeziorny constant, Z_t (as same value as K_A from the Avrami equation, which indicates the rate of crystallization of Avrami), is influenced by the cooling rate (φ). So, the crystallization rate constant (Z_c) in non-isothermal crystallization can be validated by having the cooling rate term as shown in following Eq. (8):

$$\ln(Z_c) = \ln(Z_t)/\varphi \quad (8)$$

Non-isothermal crystallization kinetics based on the Ozawa model [12, 13, 19, 20]

A theoretical model of Ozawa was used to describe the non-isothermal crystallization kinetics by developing the theoretical models of Avrami from the assumption that the non-isothermal crystallization process is a small step of isothermal crystallization. The fractional crystallinity (α) at time t is shown in following Eq. (9):

$$\alpha(t) = [1 - \exp(-K_o^m/\varphi)] \quad (9)$$

where K_o is Ozawa crystallization rate which depends on temperature, φ is cooling rate, and m is Ozawa constant. In general, this equation is often converted to the traditional linear form as following Eq. (10):

$$\ln[-\ln(1 - \alpha(t))] = \ln(K_o) - m \ln(\varphi) \quad (10)$$

where m and K_o values are obtained from the slope and interception on the y -axis of the graph from the relationship between $\ln[-\ln(1 - \alpha(t))]$ versus $\ln(\varphi)$, respectively.

Experimental

Materials

Poly(lactic acid) (PLA), trade name is Ingeo^{IM} Biopolymer 2003D (NatureWorks, Purac, Netherlands) with a number-average molecular mass of 61,000 as determined by dilute-

solution viscosity measurements in chloroform at 25 $^{\circ}\text{C}$. The PLA pellets were translucent and semi-crystalline with glass transition temperature (T_g) of 61 $^{\circ}\text{C}$ and melting temperature (T_m) of 156 $^{\circ}\text{C}$. Poly(butylene succinate) (PBS), trade name is GS Pla[®] FZ91PD (Mitsubishi Chemical Corporation, China). The PBS pellets were milky white color with a number-average molecular mass of 30,000 and T_g of -30 $^{\circ}\text{C}$ and T_m of 110 $^{\circ}\text{C}$. As a nucleating agent, talc (Talcum powder) was obtained from Sigma-Aldrich with a molecular mass of 379.27 g mol^{-1} .

Preparation of PLA/PBS blends with talc by melt blending

PLA and PBS powders were prepared by using grinder and dried in a vacuum oven for 24 h at 70 $^{\circ}\text{C}$, prior to use. Then, PLA and PBS were weighed in glass container in ratio of 90/10 by mass and mixed with talc 0.1% of polymer mass. The mixtures were heated at a temperature of 180 ± 5 $^{\circ}\text{C}$ and stirred using high-torque mechanical stirrer with a speed of 40 rpm, under nitrogen gas atmosphere, for 20 min in nitrogen atmosphere until the blend was melted homogeneously. The blend was then taken from the glass container, cut it into small pieces and keep in desiccator before further use.

Characterization

Isothermal crystallization kinetics

Differential scanning calorimetry (DSC, Perkin-Elmer Pyris 7) was used as a tool to observe the isothermal crystallization characteristics. A sample (10 ± 1 mg) was put into an aluminum pan and hermetically sealed. The samples were then heated from 20 to 200 $^{\circ}\text{C}$ at a heating rate of 20 $^{\circ}\text{C min}^{-1}$ and maintained at this temperature for 2 min to remove the thermal history. Subsequently, the sample was quenched to 20 $^{\circ}\text{C}$ at a cooling rate of 10 $^{\circ}\text{C min}^{-1}$, reheated to 200 $^{\circ}\text{C}$ at a heating rate of 10 $^{\circ}\text{C min}^{-1}$, and hold for 2 min. For the kinetic study, the sample was quenched to desired crystallization temperatures; 70, 80, 90, 100, 110 and 120 $^{\circ}\text{C}$. They were held at each isothermal temperature to allow the complete crystallization. Moreover, the melting behavior of the isothermally crystallized samples was observed by reheating to 200 $^{\circ}\text{C}$ at a rate of 10 $^{\circ}\text{C min}^{-1}$ in a nitrogen atmosphere.

Non-isothermal crystallization kinetics

To observe the non-isothermal crystallization characteristics, a sample (10 ± 1 mg) was put into an aluminum pan and hermetically sealed. The samples were then heated from 20 to 200 $^{\circ}\text{C}$ at a heating rate of 20 $^{\circ}\text{C min}^{-1}$ and

maintained at this temperature for 2 min to remove the thermal history. Subsequently, the samples were quenched to 20 °C at a cooling rate of 5, 10, 20, 40, 60, 80 and 100 °C min⁻¹ and reheated to 200 °C at a rate of 10 °C min⁻¹ in a nitrogen atmosphere.

Results and discussion

Isothermal crystallization behaviors

Figure 1 shows DSC curves of the PLA/PBS blends with 0.1% by mass of talc at isothermal temperatures of 70, 80, 90, 100, 110 and 120 °C. And, Fig. 2 shows DSC melting curves of the PLA/PBS blends with 0.1% by mass of talc after isothermal crystallization at various temperatures. The results show that the different isothermal temperatures gave the different crystallization times and the amounts of crystallinity. There was no exothermic peak at isothermal temperature at 70 and 80 °C. This suggests that no crystalline occurred at these temperatures. It corresponds to their DSC melting curves which the endothermic peaks of the crystallization were observed, implying the crystalline occurred during heating. On the other hand, at the isothermal temperatures of 90, 100, 110 and 120 °C, it can be seen the clear exothermic peak, resulting from the crystallization. From Fig. 1, it indicates that the completion of the crystallization blending process at 100 °C took the shortest time which compared to those of the other isothermal temperatures.

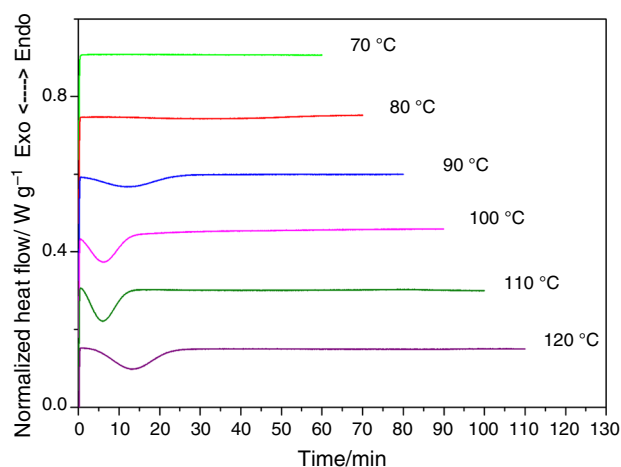


Fig. 1 The DSC curves of the PLA/PBS blends with 0.1% by mass of talc at isothermal temperatures of 70 °C, 80 °C, 90 °C, 100 °C, 110 °C, and 120 °C

Isothermal crystallization kinetics based on the Avrami model

The integral crystallization curves of the PLA/PBS blends with 0.1% by mass of talc at the various isothermal crystallization temperatures are shown in Fig. 3. The percentage relative of crystallinity increased when the crystallization time was increased. At 100 °C isothermal temperature, the crystallization process occurred earlier and gave the highest crystallization rate. This gave similar result for 110 °C isothermal temperature. Nevertheless, the crystallization process and the crystallization rate decreased at 120 °C isothermal temperature significantly. The Avrami parameters, Avrami exponents (n_A), Avrami crystallization rate (K_A) and half-time of crystallization

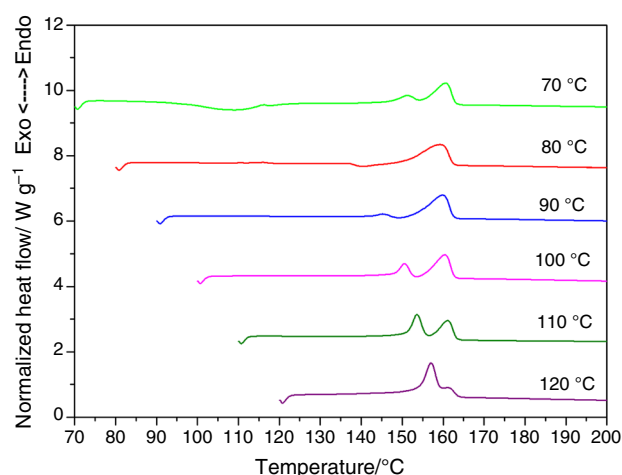


Fig. 2 The DSC melting curves of the PLA/PBS blends with 0.1% by mass of talc after isothermal crystallization at the various temperatures

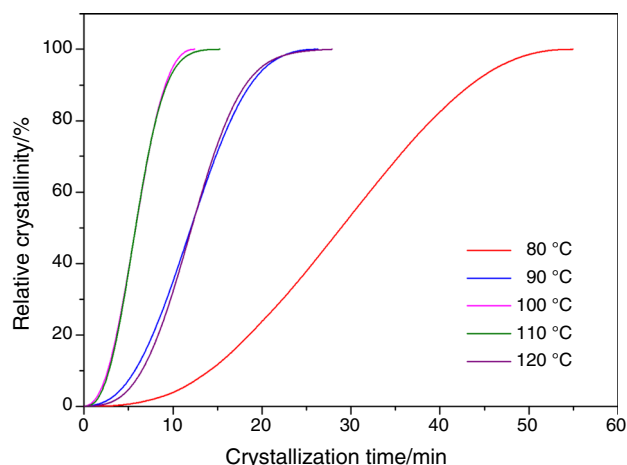


Fig. 3 The integral crystallization curves (based on the Avrami model) of the PLA/PBS blends with 0.1% by mass of talc at the various isothermal crystallization temperatures

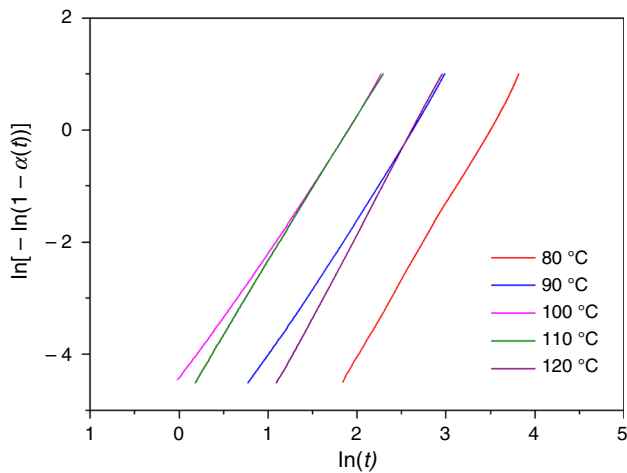


Fig. 4 The plot of $\ln[-\ln(1 - \alpha(t))]$ versus $\ln(t)$ of the PLA/PBS blends with 0.1% by mass of talc at the various isothermal crystallization temperatures (based on the Avrami model)

($t_{1/2}$) were estimated from $\ln[-\ln(1 - \alpha(t))]$ versus $\ln(t)$ plot and are shown in Fig. 4 and Table 1.

The n_A value is dependent upon the growth dimension and type of nucleation. From Table 1, the average n_A value was 2.6 which close to 3 which indicated that spherulitic growth from instantaneous nuclei of heterogeneous nucleation and it occurred from additive. The n_A value increased from 2.3 to 2.9 with increasing temperatures is possibly also due to the type of crystal growth from 2 to 3 growth dimension [21]. The higher K_A value means faster crystallization process and the highest K_A is found to be at 100 °C. The half-time of crystallization ($t_{1/2}$) showed the minimum value at the same temperature, 100 °C and gave the highest growth rate as in Fig. 5.

Isothermal crystallization kinetics based on the Tobin model

The Tobin parameters were calculated from the plots of $\log(\alpha_t/(1 - \alpha_t))$ versus $\log(t)$, as shown in Fig. 6. Tobin's isothermal crystallization kinetic parameters of PLA/PBS blends with 0.1% by mass of talc are shown in Table 2. The n_T and K_T values were obtained from the slope and interception. The n_T value increased from 2.9 to 3.2 with increasing isothermal temperatures. The highest K_T is found to be at 100 °C, which is similar as Avrami model. The half-time of crystallization ($t_{1/2}$) showed the minimum value at 100 and 110 °C and gave the highest growth rate as in Fig. 7. Tobin parameters had the trends as similar as Avrami parameters.

Table 1 Avrami's isothermal crystallization kinetic parameters of PLA/PBS blends with 0.1% by mass of talc

Temperature/°C	n_A	K_A/min^{-1}	$t_{1/2}/\text{min}$	G/min^{-1}
80	2.7	6.87×10^{-5}	28.3	0.035
90	2.5	1.30×10^{-3}	11.9	0.084
100	2.3	1.14×10^{-2}	5.7	0.175
110	2.6	6.72×10^{-3}	5.8	0.170
120	2.9	4.58×10^{-4}	12.2	0.082

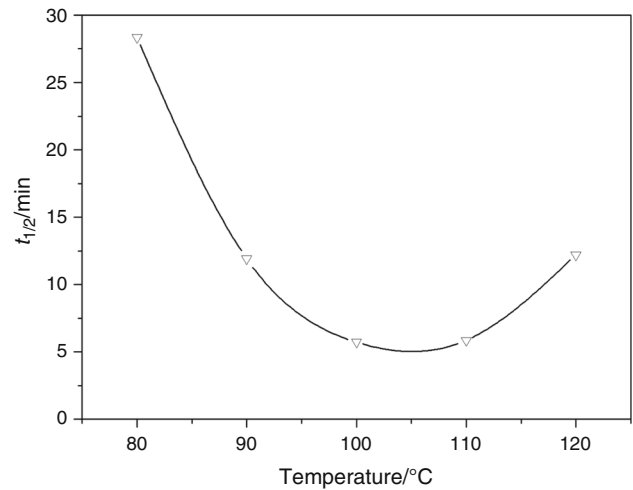


Fig. 5 The effect of talc on the half-time of crystallization as a function of the isothermal temperature (based on the Avrami model)

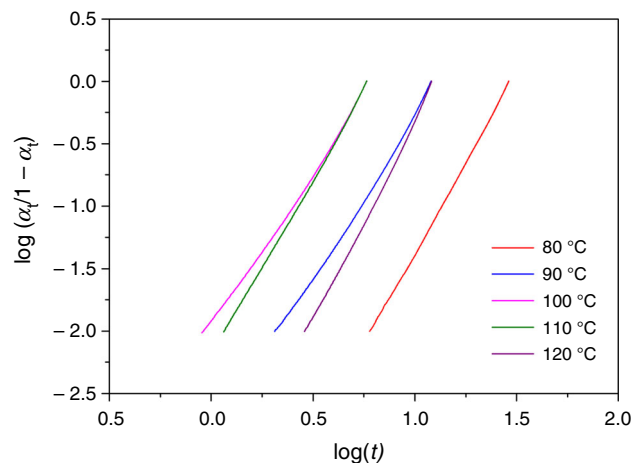


Fig. 6 The plot of $\log(\alpha_t/(1 - \alpha_t))$ versus $\log(t)$ of the PLA/PBS blends with 0.1% by mass of talc at the various isothermal crystallization temperatures (based on the Tobin model)

Non-isothermal crystallization behaviors

From Fig. 8, the results showed that the crystallization peaks of PLA/PBS blends with 0.1% by mass of talc shifted to lower temperature as the cooling rate increased.

It was possibly due to the crystallization at the lower cooling rate had enough time to crystallize, and the nucleation and crystal growth crystallized at a higher temperature with narrower range. On the other hand, at

Table 2 Tobin's isothermal crystallization kinetic parameters of PLA/PBS blends with 0.1% by mass of talc

Temperature/°C	n_T	K_T/min^{-1}	$t_{1/2}/\text{min}$	G/min^{-1}
80	2.9	0.013	3.8	0.26
90	2.8	0.048	2.6	0.38
100	2.6	0.133	1.9	0.53
110	2.9	0.109	1.9	0.53
120	3.2	0.029	2.7	0.37

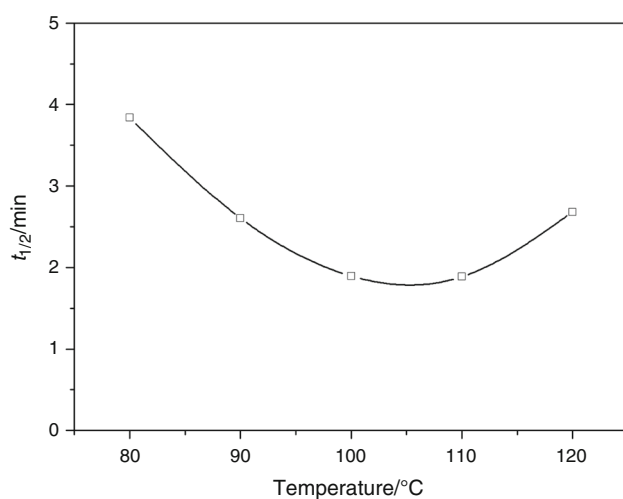


Fig. 7 The effect of talc on the half-time of crystallization as a function of the isothermal temperature (based on the Tobin model)

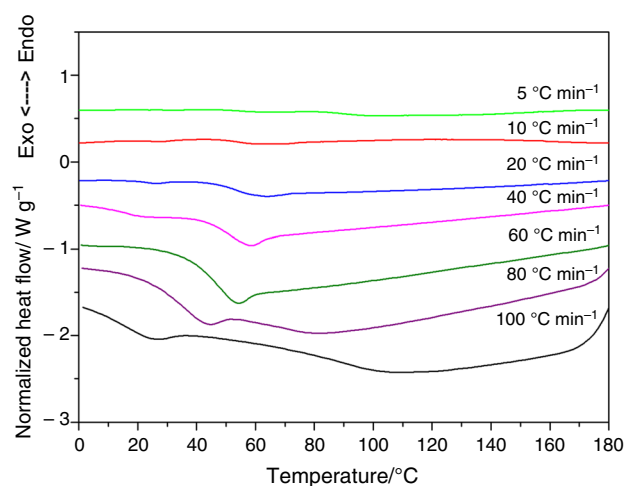


Fig. 8 The DSC curves of heat flow as a function of temperature at different cooling rates for the PLA/PBS blends with 0.1% by mass of talc

higher cooling rate, there was insufficient time for nucleation and crystal growth to crystallize. The crystallization peaks were in the wider range and the amount of crystal decreased. Cooling rate of $40\text{ }^{\circ}\text{C min}^{-1}$ gave the highest amount of crystallinity and found to be the appropriate cooling rate for this system.

Non-isothermal crystallization kinetics based on the Jeziorny model

The result from the relationship between %relative crystallinity and crystallization time is shown in Fig. 9. It can be clearly seen that the higher cooling rate and the shorter time of crystallization had affected the completion of crystallization process. The Avrami plots of $\ln[-\ln(1-X_t)]$ versus $\ln(t)$ are shown in Fig. 10. Avrami and Jeziorny parameters are determined and shown in Table 3.

As shown in Fig. 10, there are approximately two stages of crystallization. Each curve showed the straight line in the primary stage followed by the nonlinear line in the secondary stage, which was clearly at high cooling rate. Primary nucleation is the characteristic of disorganized nucleation which is expected to be caused by a number of molecules line up next to each other and from new phase. It could imply that there are two types of nucleation. The first one is the homogeneous nucleation; the creation of a nucleus implies the formation of an interface at the boundaries of a new phase at the lower temperature. The second one is heterogeneous nucleation; the nucleation normally occurs at nucleation sites on surfaces contacting the adulterated thing or nucleating agent which was filled in polymer. The secondary nucleation occurs from contacting of the existing crystal and existing crystal or the existing crystal and wall.

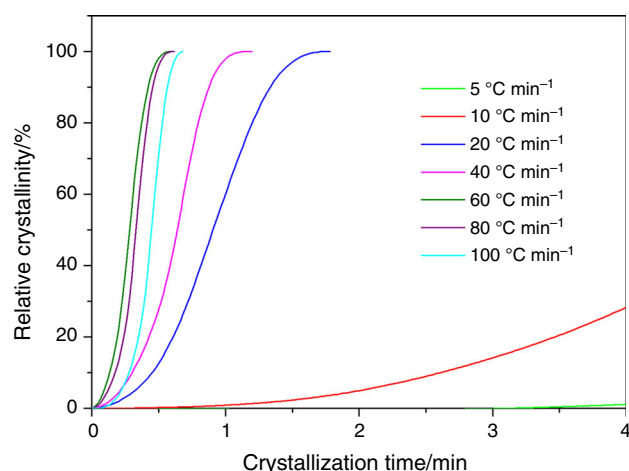


Fig. 9 The integral crystallization curves of the PLA/PBS blends with 0.1% by mass of talc at the various cooling rates

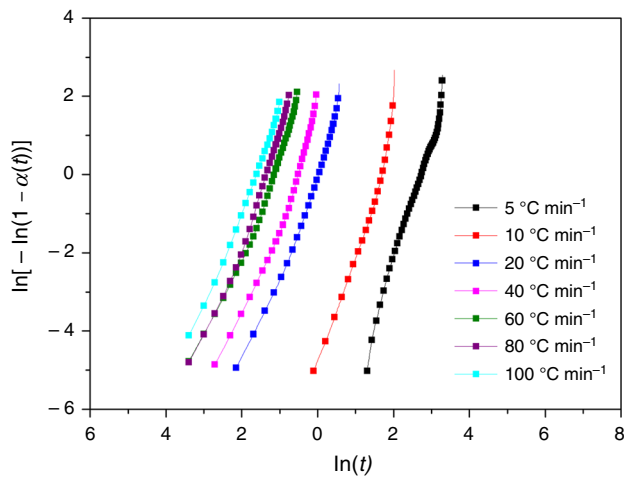


Fig. 10 The plot of $\ln[-\ln(1 - \alpha(t))]$ versus $\ln(t)$ of the PLA/PBS blends with 0.1% by mass of talc at the various cooling rates

Table 3 Avrami and Jeziorny parameters of PLA/PBS blends with 0.1% by mass of talc at various cooling rates

Cooling rate/ $^{\circ}\text{C min}^{-1}$	n_A	K_A/min^{-1}	$t_{1/2}/\text{min}$	Z_c
5	2.9	2.99×10^{-4}	13.48	0.1970
10	2.7	7.86×10^{-3}	5.14	0.6160
20	3.0	0.952	0.90	0.9975
40	3.7	6.65	0.54	1.0485
60	1.9	4.79	0.35	1.0264
80	1.8	4.66	0.36	1.0194
100	1.8	9.74	0.24	1.0230

In Table 3, there are various values of n_A . Zou et al. reported that there are two factors which affect the value of n . The first one is due to the fast crystallization rate of polymer at high cooling rate prevents the development of spherulites, resulting a decrease in the n value. The other one is the growth site impingement of spherulites and secondary crystallization may change the crystallization mechanism [22]. Jeziorny crystallization rate and the half-time of crystallization ($t_{1/2}$) showed a similar trend as Avrami model. Jeziorny crystallization rate increased when the cooling rate was increased. Nevertheless, at higher temperature was affected by secondary crystallization as n value.

Non-isothermal crystallization kinetics based on the Ozawa model

Figure 11 shows the plot $\ln[-\ln(1 - \alpha(t))]$ versus $\ln(\phi)$. Normally, n and K value should have calculated from the straight line. In this study, all curves are nonlinear. This suggests that Ozawa parameters could not be calculated.

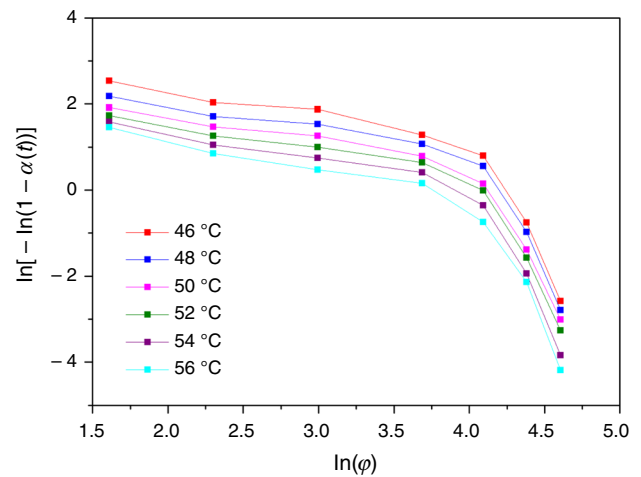


Fig. 11 The plot of $\ln[-\ln(1 - \alpha(t))]$ versus $\ln(\phi)$ of the PLA/PBS blends with 0.1% by mass of talc at the various crystallization temperatures

Moreover, there is no explaining about changing of the crystallization mechanism which includes primary and secondary nucleation [12]. It indicated that Ozawa model was inappropriate for describing the non-isothermal crystallization of these systems.

Conclusions

In this work, the blends of PLA/PBS with 0.1% by mass of talc were prepared by melt blending to optimize on the isothermal and non-isothermal crystallization kinetics. From the isothermal crystallization kinetic results indicated that the completion of the crystallization blending process at 100 °C took the shortest time. The Avrami parameters were estimated from the various isothermal crystallization temperatures and the results show that the lowest half-time of crystallization was performed at 100 °C isothermal temperature. It could be suggested that at 100 °C isothermal temperature was a suitable temperature for a cycle time for PLA/PBS for crystallization. The smaller the $t_{1/2}$ value exhibited the higher the crystallization rate. The Tobin parameters were also estimated and it shows that the n_T value has higher value than that of n_A approximately about 0.3. Moreover, Tobin parameters had the trends as similar as Avrami parameters.

From the non-isothermal crystallization kinetic results indicated that the crystallization peaks shifted to lower temperature when the cooling rate increased. Nevertheless, at higher cooling rate, there was insufficient time for nucleation and crystal growth to crystallize. So, the crystallization peak was wider, and the amount of crystal was lower. Cooling rate of 40 °C min^{-1} gave the highest amount of crystallinity and was found to be the appropriate

rate for this condition. Non-isothermal crystallization kinetics based on the Jeziorny model indicated that there are two stages of crystallization which are straight line in the primary stage followed by the nonlinear line in the secondary stage, which was clearly at high cooling rate. Jeziorny crystallization rate and the half-time of crystallization showed a similar trend as Avrami model. Jeziorny crystallization rate increased when the cooling rate was increased. Nevertheless, at higher temperature was affected by secondary crystallization as indicated by n value. It was also found that Ozawa model was inappropriate for describing the non-isothermal crystallization of these systems. Based on current finding, talc is suitable to be the nucleating agent for PLA/PBS blends. This study provides useful information on the polymer processing which could estimate the reduction of the crystallization time and may enable its wider applications.

Acknowledgements This research work was partially supported by Chiang Mai University. Authors would like to thank Department of Chemistry, Chiang Mai University, for providing the research facilities used.

Compliance with ethical standards

Conflict of interest The authors declare that they have no conflict of interest.

References

1. Tsuji H. Poly(lactic acid) stereocomplexes: a decade of progress. *Adv Drug Deliv Rev.* 2016;107:97–135.
2. Karamanlioglu M, Preziosi R, Robson GD. Abiotic and biotic environmental degradation of the bioplastic polymer poly(lactic acid): a review. *Polym Degrad Stab.* 2017;137:122–30.
3. Sonchaeng U, Iñiguez-Franco F, Rafael Auras SS, Rubino M, Lim L-T. Poly(lactic acid) mass transfer properties. *Prog Polym Sci.* 2018;86:85–121.
4. Chavalitpanyaa K, Phattananudee S. Poly(lactic acid)/polycaprolactone blends compatibilized with block copolymer. *Energy Procedia.* 2013;34:542–8.
5. Patrício T, Bártolo P. Thermal stability of PCL/PLA blends produced by physical blending process. *Procedia Eng.* 2013;59:292–7.
6. Signoria F, Coltelli M-B, Bronco S. Thermal degradation of poly(lactic acid) (PLA) and poly(butylene adipate-co-terephthalate) (PBAT) and their blends upon melt processing. *Polym Degrad Stab.* 2009;94(1):74–82.
7. Pivsa-Art W, Pavasupree S, O-Charoen N, Insuan U, Jailak P, Pivsa-Art S. Preparation of polymer blends between poly (L-lactic acid), poly (butylene succinate-co-adipate) and poly (butylene adipate-co-terephthalate) for blow film industrial application. *Energy Procedia.* 2011;9:581–8.
8. Hassan E, Wei Y, Jiao H, Muho Y. Dynamic mechanical properties and thermal stability of poly(lactic acid) and poly(-butylene succinate) blends composites. *J Fiber Bioeng Inform.* 2013;6:85–94.
9. Bhatia A, Gupta RK, Bhattacharya SN, Choi HJ. Compatibility of biodegradable poly (lactic acid) (PLA) and poly (butylene succinate) (PBS) blends for packaging application. *Korea Aust Rheol J.* 2007;19:125–31.
10. Li H, Huneault MA. Effect of nucleation and plasticization on the crystallization of poly(lactic acid). *Polymer.* 2007;48:855–6866.
11. Battagazzore D, Bocchini S, Frache A. Crystallization kinetics of poly(lactic acid)-talc composites. *Express Polym Lett.* 2011;5:849–58.
12. Deshmukh GS, Peshwe D, Pa SU, Ekhe JD. Nonisothermal crystallization kinetics and melting behavior of poly(butylene terephthalate) (PBT) composites based on different types of functional fillers. *Thermochim Acta.* 2014;581:41–53.
13. Meng Z, Yang L, Geng W, Yao Y, Wang X, Liu Y. Kinetic study on the isothermal and nonisothermal crystallization of monoglyceride organogels. *Sci World J.* 2014;2014:1–7.
14. Bosq N, Aht-Ong D. Isothermal and non-isothermal crystallization kinetics of poly(butylene succinate) with nanoprecipitated calcium carbonate as nucleating agent. *J Therm Anal Calorim.* 2018;132(1):233–49.
15. Nikam PN, Deshpande VD. Isothermal crystallization kinetics of PET/alumina nanocomposites using distinct macrokinetic models. *J Therm Anal Calorim.* 2019. <https://doi.org/10.1007/s10973-019-08192-x>.
16. Supaphol P, Spruiell JE. Avrami, Tobin, Malkin, and simultaneous Avrami microkinetic models to isothermal crystallization of syndiotactic polypropylenes. *J Macromol Sci Phys.* 2000;B39(2):257–77.
17. Jeziorny A. Parameters characterizing the kinetics of the non-isothermal crystallization of poly(ethylene terephthalate) determined by d.s.c. *Polymer.* 1978;19:1142–4.
18. Saad GR, Elsayw MA, Aziz MSA. Nonisothermal crystallization behavior and molecular dynamics of poly(lactic acid) plasticized with jojoba oil. *J Therm Anal Calorim.* 2017;128(1):211–23.
19. Sajkiewicz P, Carpaneto L, Wasiak AL. Application of the Ozawa model to non-isothermal crystallization of poly(ethylene terephthalate). *Polymer.* 2001;42:5365–70.
20. Li Y, Han C, Yu Y, Xiao L, Shao Y. Isothermal and non-isothermal cold crystallization kinetics of poly(L-lactide)/functionalized eggshell powder composites. *J Therm Anal Calorim.* 2018;131(3):2213–23.
21. Cai J, Liu M, Wang L, Yao K, Li S, Xiong H. Isothermal crystallization kinetics of thermoplastic starch/poly(lactic acid) composites. *Carbohydr Polym.* 2011;86(2):941–7.
22. Zou P, Tang S, Fu Z, Xiong H. Isothermal and non-isothermal crystallization kinetics of modified rape straw flour/high-density polyethylene composites. *Int J Therm Sci.* 2009;48:837–46.

Publisher's Note Springer Nature remains neutral with regard to jurisdictional claims in published maps and institutional affiliations.